Aerodynamic Effect of Forewing-Hindwing Interactions in Hovering and Forward Flight of Dragonfly

Flight of Dragonfly

Zheng Hu and Xinyan Deng*

Department of Mechanical Engineering, University of Delaware, 126 Spencer Laboratory, Newark, DE 19716, USA.

* To whom correspondence should be addressed. Email: deng@udel.edu

Summary

Dragonflies move each wing independently and therefore may alter the phase difference (γ) between the forewing and hindwing stroke cycles. They are observed to change the phase difference for different flight modes. We investigated the aerodynamic effect of phase difference during hovering and forward flight with a 60° inclined stroke plane by using a pair of dynamically scaled robotic dragonfly model wings. Aerodynamic forces were measured while phase difference was systematically varied. The results showed that, i) for hovering flight, $\gamma=0°$ enhanced the lift force on both forewing and hindwing; $\gamma=180°$ was detrimental for lift generation, but was beneficial for vibration suppression and body stabilization. This result may help understand the dragonfly behavior that 0° was used in acceleration mode while 180° was used in hovering mode. ii) For forward flight, wing-wing interaction was always beneficial for forewing lift while detrimental for hindwing lift; the total lift was only slightly reduced when $\gamma=0\sim90°$ and significantly decreased by 38% when $\gamma=270°$. This result may explain why dragonflies employ 50~100° during forward flight, while 270° is never favored. Thrust force was also reduced by wing-wing interaction to some extent. We experimentally investigated the wing-wing interaction mechanism and measured two types of interaction flow: sharp upwash and mild flow. The former was caused by the leading edge vortex (LEV) of hindwing and resulted in lift enhancement on the forewing, while the latter is a kind of local flow interaction which resulted in either an upwash or downwash.

Introduction

Dragonfly is one of the most maneuverable insects and one of the oldest flying species on earth. Their flight performance far exceeds other insects. They can hover, cruise up to 54km/h, turn 180° in three wing beats, fly sideways, glide, and even fly backwards (Alexander, 1984; Appleton, 1974; Whitehouse, 1941). They intercept prey in the air with amazing speed and accuracy. Their thorax are equipped with wing muscles which accounts for 24% (*Aeshna*) of its body weight, compared to 13% of those of the honey bees (Appleton, 1974). Most dragonflies change their wing motion kinematics for different flight modes such as hovering, cruising and turning. Among these kinematic parameters, the most interesting one is the phase difference (γ) between forewing and hindwing. It is defined as the phase angle by which the hindwing leads the forewing. When hovering, dragonflies employ 180° phase difference (anti-phase) (Alexander, 1984; Norberg, 1975; Rüppell, 1989), while 54~100° are used for forward flight (Azuma and Watanabe, 1988; Wang et al., 2003). When accelerating or performing aggressive maneuvers, they use 0° (in-phase) phase difference (Alexander, 1984; Rüppell, 1989; Thomas et al., 2004). Of various phase differences, 270° is rarely observed in dragonfly flight.

The fact that flapping in-phase (0°) appears in situations requiring large acceleration suggests that in-phase might produce higher forces (Alexander, 1984; Rüppell, 1989). The film sequences made by Alexander (Alexander, 1984) showed that in-phase is employed during take-off and sharp turning. It was also found that in a rising flight of a dragonfly, lift was increased during downstroke and drag was increased during upstroke when flying in-phase (Azuma et al., 1985). The conclusion was derived by using

3

the momentum theory and the blade element theory, combined with a numerical method modified from the local circulation method.

However, it was argued that as two wings in tandem are brought closer together, the lift force produced by each wing is reduced (Alexander, 1984). Therefore, forewing and hindwing flapping in-phase would produce less lift because they are closer together than when beating anti-phase. Alexander believed that the reason of dragonflies using in-phase flight may be due to physiological reason as well as the preference of peak forces enhancement at the cost of the mean forces reduction (Alexander, 1984).

Counterstroking (180° or anti-phase) produces uniform flight, whereas flight produced by parallel stroking (0°) is irregular (Rüppell, 1989). This is because inequalities in the aerodynamic effects of the upstroke and downstroke can be compensated to some extent in countertroking (Fig. 7). As one pair of wing's upstroke with a steep angle of attack generates strong thrust, the other pair's downstroke with a small angle of attack mainly generates lift. Therefore the net thrust and lift production remains relatively constant during flight due to the alternating force generation on two wings (Rüppell, 1989).

In a recent computational study, (Wang and Russell, 2007) calculated dragonfly's aerodynamic force and power as a function of forewing-hindwing phase difference. They found that anti-phase flapping consumes nearly minimal power while generating sufficient force to balance body weight, and that in-phase motion provides an additional force to accelerate (Wang and Russell, 2007). Furthermore, they proposed an analogy to explain the results by analyzing a model of two cylinders moving in parallel next to each other.

Other computational studies include (Wang and Sun, 2005) and (Huang and Sun, 2007), where they calculated the aerodynamic effects of forewing-hindwing interactions of a specific dragonfly (*Aeshna juncea*) in hover and slow forward flight. They showed that the interaction is detrimental to force generation in almost all cases. At hovering with $\gamma=180°$, the reduction is 8~15%, compared with the force without interaction. The force on hindwing is greatly influenced by the forewing at $\gamma=180~360°$, with the lift coefficient decreased by 20~60%. Furthermore, they proposed a mechanism to explain the effect of forewing on hindwing force reduction: the forewing in each of its downstroke produces a downward "jet" behind it; when the hindwing lags the forewing, it moves into the jet and its effective angle of attack is reduced, resulting in a decrease in its aerodynamic force.

Previous computational studies include (Lan, 1979), where the unsteady quasi-vortex-lattice method was applied to the study of dragonfly aerodynamics, and the results showed that dragonfly can produce high thrust with high efficiency if hindwing leads the forewing by 90°, and that hindwing was able to extract wake energy from the forewing under this condition.

Direct force measurements on tethered dragonflies showed that peak lift increases from approximately 2 to 6.3 times body weight when the animal decreases the phase difference between both flapping wings (Reavis and Luttges, 1988). But maybe this enhancement on peak lift may due to overlap of peak lifts on forewing and hindwing, not necessarily due to wing-wing interaction.

Experimental investigations of the aerodynamic effect of wing-wing interaction was previously performed in (Maybury and Lehmann, 2004), where a pair of robotic

wings were vertically stacked to simulate dragonfly hovering flight with horizontal stroke plane. They found that the lift production of the forewing remains approximately constant, while hind wing lift production is reduced to some extent and its maximum value occurs at a phase difference $\gamma = 90°$. They attributed the wing-wing interaction to two reasons: LEV destruction and local flow condition (Maybury and Lehmann, 2004). Their results explained the hovering behavior of dragonflies using horizontal stroke plane (*Sympetrum Sanguineum*), while many other dragonfly species employ a 20~70° inclined stroke plane (Alexander, 1984; Norberg, 1975; Rüppell, 1989) and employ an aerodynamic mechanism of "drag based lift generation" (Wang, 2004), which is quite different from that for horizontal stroke plane flight (Wang and Russell, 2007). In this study, we investigate the wing-wing interaction and the underlying mechanism for the inclined stroke plane species.

As we can see, the effect of the forewing-hindwing interactions in dragonflies has been investigated with some computational and experimental studies, but conclusions are still limited and quite varying. In this study, we constructed a pair of robotic dragonfly wings to investigate the aerodynamic effect of wing-wing interactions in both hovering and forward flight. This apparatus enables us to study inclined stroke plane species such as *Aeshna Juncea* with an inclined stroke plane 60° and varying forward speed. The wing bases are of close proximity to mimic the dragonfly wings. We systematically vary the different phase between the forewing and hindwing to find out why dragonflies apply certain phase differences rather than others in certain flight modes. Furthermore, to investigate the underlying fluid interaction mechanism, we conducted rod based experiments to detect downwash or upwash flow from a neighboring wing.

Materials and methods

Experimental Setup

We constructed a pair of dynamically-scaled robotic wings to replicate dragonfly wing motion and measure the instantaneous aerodynamic forces and torques (Fig. 1A). Briefly, we used a pair of bevel-geared robotic wrists to generate rotational motion in three independent degrees of freedom. For each wing, a set of bevel gears transmits the motion from coaxially driven shafts to the wing holder thus enabling wing flapping, rotation and deviation. Since the deviation angles are quite small and their effects on aerodynamic forces are minimal (Dickinson et al., 1999), we have further modified the gearbox to take out the deviation DoF (degree of freedom) and were therefore able to mount the wing bases with sensors inside the gearbox. By doing so the wing bases coincide with the intersection of the rotational axis and the two wings are of very close proximity like those of the dragonflies. In addition, the two flappers are mounted on a linear stage driven by a stepper motor to achieve forward motion together (Fig. 1A).

The drive shafts were powered by 16 mm, 0.3 Nm torque DC brush motors (Maxon, Sachseln, Switzerland) equipped with gear heads to reduce speed and magnetic encoders to provide kinematic feedback to ensure motion fidelity. The motors were driven along kinematic patterns provided by a custom MATLAB (Mathworks, Natick, MA) Simulink program with WinCon software (Quanser Consulting, Ontario, Canada). This software provided commands to the real-time control and data acquisition board (Quanser Consulting, Ontario, Canada) communicating with the hardware. We used Proportional-Integral-Derivative (PID) controllers to run the motors with precision of 0.1^{o}. Motion commands from the computer were amplified by analog amplifier units

(Advanced Motion Control) which directly controlled the input current received by the motor.

The wing models were made from Mylar plastic film with a thickness of 0.25 cm which behaves as a rigid wing in our experiments. A carbon fiber rod was glued on the plastic film to serve as the leading edge. The end of the carbon fiber rod was affixed on to the force sensor. The wings have identical geometry as the dragonfly wings but are four times larger with a length of 19 cm for forewing and 18.5 cm for hindwing. The wing length is calculated as the distance from wing tip to the flapping axis. For the gear boxes, we adopted an improved design to reduce the null space resulting from gear box, force sensor and wing holder to only 1 cm (Fig. 1B). The two wings are put together at a close proximity without touching each other when moving (Fig. 1B).

The wing models along with the gearboxes are immersed into a tank (46 cm by 41 cm by 152 cm) filled with mineral oil (Kinematic viscosity= 3.4 cSt at 20°C, density=830 kg/m^3). This overall set-up enabled us to move the wings along pre-determined dragonfly kinematic patterns while simultaneously measuring the forces on the forewing and the hindwing respectively (Fig. 1A).

In order to cover the whole scope of phase differences, we systematically varied the phase difference between forewing and hindwing in steps of 30°. Next, to prove the existence of downwash or upwash generated by a wing, we mount a stationary thin rod equipped with the same sensor in place of the other wing to sense the flow generated by the moving wing (Fig. 4).
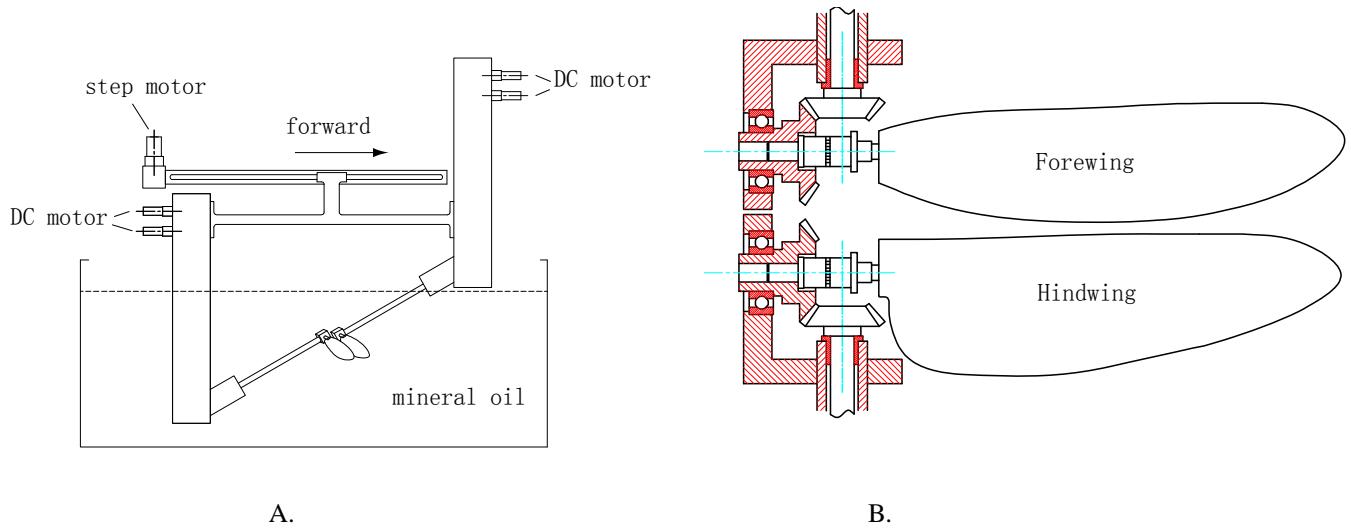
Fig. 1. Sketch of experimental setup: A. Overall setup; B. wing hinge design

Flight data of Aeshna juncea

High-speed photos of the dragonfly (*Aeshna juncea*) in hovering flight were taken by Norberg (Norberg, 1975). The body is held almost horizontal, and the wing stroke plane is tilted 60° (*β*) relative to the horizontal line. For both forewing and hindwing, the chord is almost horizontal during the downstroke and is close to being vertical during the upstroke (Fig. 2); the stroke frequency (*n*) is 36 Hz, the stroke amplitude (Φ) is 60°; the translational angle (ϕ_f) is from 35° above the horizontal to 25° below for forewing, and (ϕ_f) is from 45° above to 15° below for hindwing; the hindwing leads the forewing in phase by 180°. The mass of the insect (*m*) is 754mg; forewing length (r_f) is 4.74 cm; hindwing length (r_h) is 4.60 cm; the mean chord lengths of the forewing and hindwing are 0.81 cm and 1.12 cm, respectively; the moment of inertial of wing-mass with respect to the fulcrum (I_f) is 4.54 $g\,cm^{-2}$ for the forewing and 3.77 $g\,cm^{-2}$ (I_h) for the hindwing (Norberg, 1972).
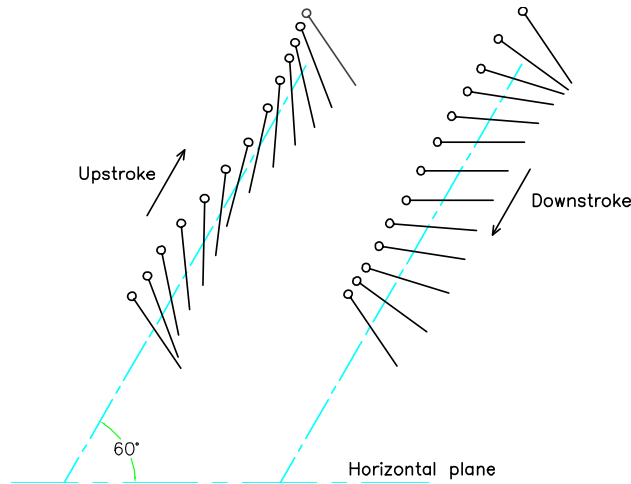
9

Fig. 2. Sketches of the dragonfly wing kineamtics during upstroke and downstroke based on Aeshna juncea data (Norberg, 1975). Side views with circles denote the leading edge. Both forewing and hindwing apply.

Due to the low frame rate of the camera used at that time (80 Hz), Norberg's data does not consist of a detailed continuous trajectory of the wing kinematics. Azuma instead, (Azuma et al., 1985) successfully filmed a slow climbing flight of a dragonfly (*Sympetrum Frequens*) with a high speed camera (873 frames per second). He showed that the flapping trajectory can be well represented by a sinusoidal function and the rotation trajectory can be represented by a third harmonic function. Since the two species (*Aeshna juncea* and *Sympetrum frequens*) share similar values for many kinematic parameters such as translational amplitude, rotational amplitude and stroke plane angle (Norberg, 1975; Azuma et al., 1985), here we assume they also employ similar wing motion trajectories. This assumption of kinematic trajectories can be reasonably applied to other species with highly inclined stroke planes without affecting the main results of this study. We developed a pair of wing kinematic trajectories by matching those for *Sympetrum Frequens* in (Azuma et al., 1985), as shown in Fig 3.
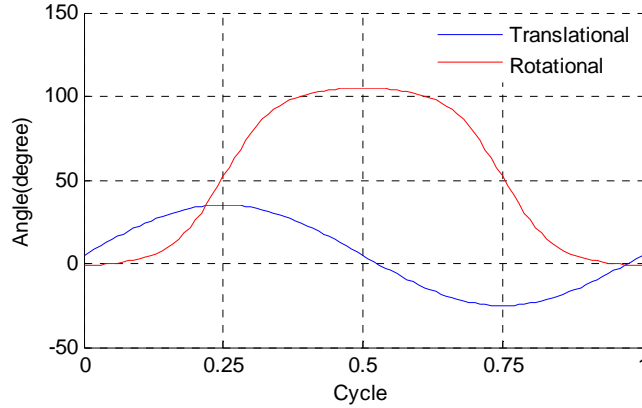
Fig. 3. Wing kinematics developed by matching those for *Sympetrum Frequens* from (Azuma et al., 1985) and (Norberg, 1975). Translational angle (blue) and rotation angle (red). This is for forewing only; the kinematics for hindwing is almost the same except a 10° offset for translational angle.

Although Norberg (Norberg, 1975) did not provide the kinematics in forward flight, he pointed out that in forward flight, the body is also kept horizontal, and horizontal and vertical winds seem not to have imposed any significant errors on the data. Therefore, we assume that in forward flight, the stroke plane is also kept around 60°, frequency is still around 36 Hz, and stroke angle does not change significantly. The changed parameter might be the angle of attack. Similar to the method used in (Wang and Sun, 2005) in the CFD study, we will also adjust the angle of attack to achieve force balance on dragonfly body weight.

Based on the dragonfly morphological and kinematics data, the mean linear velocity of the wing is $U = 2\Phi n r_2 = 2.1 \text{ms}^{-1}$, and the Reynolds number is calculated to be $Re = Uc / \upsilon \approx 1160$.

Force measurement and inertial subtraction

For each wing, we measured the instantaneous lift and thrust forces and calculated the average forces. The forces as well as torques on the moving wings can be measured by a six-component force sensor (ATI NANO-17, Apex, NC), with a range of ±12 N for force and ±0.5 Nm for torque along three orthogonal axes. Using appropriate trigonometric conversions, these force measurements were then converted to lift and thrust forces in the earth coordinates. Note that in this study, lift force is defined as the vertical component of the aerodynamics force on the wing and thrust force is the horizontal component in global coordinate frame.

The force measured from the sensor is a combination of wing aerodynamic force, wing (plus wing holder) gravity (plus buoyancy in oil) and wing inertial force. To extract the aerodynamic information from the raw data, we first subtract the gravity (plus buoyancy in oil) of wing (plus wing holder). This can be done straightforwardly by measuring the weight of gravity of wing (plus wing holder) in oil. The next step is to subtract the inertial force component. We estimated the contribution of wing inertial forces analytically, assuming that all mass of the wing (m_w) is concentrated in the wing center of mass. m_w is 1.5 g. The inertia force along the stroke plane direction caused by translational acceleration is calculated as follows, similar to (Maybury and Lehmann, 2004):

$$F_x^*(t) = m_w l_x \ddot{\phi} \qquad\qquad (1)$$

in which l_x is the first moment arm, t is time, $\ddot{\phi}$ is the translational angular acceleration, which is a sinusoidal function with amplitude of 10 rad/s^{-2}. We found the distance

between the rotation axis and the wing's gravity center l_x experimentally. The magnitude of the wing inertia force in our experiment $F_x^*(t)$ is 1.7×10^{-3} N, which counts for less than 1% of the total force measured by the sensor. Since the distance from wing center of mass to its rotational axis l_y is much shorter than the distance to its translational axis l_x, the inertia force components caused by rotational acceleration can be neglected.

Force scaling and force coefficient calculation

The magnitude of aerodynamic forces acting on an actual dragonfly, F_{fly}, is related to those measured in the robotic model, F_{robot}, according to the following scaling rule (Fry et al., 2005):

$$F_{fly} = F_{robot} \cdot \frac{\rho_{air}}{\rho_{oil}} \cdot \left(\frac{n_{fly}}{n_{robot}} \right)^2 \cdot \left(\frac{r_{fly}}{r_{robot}} \right)^2 \cdot \frac{S_{fly}}{S_{robot}} \cdot \frac{\hat{r}_{2fly}^2}{\hat{r}_{2robot}^2} \tag{2}$$

where ρ is fluid density, n is stroke frequency, r is wing length, S is wing area, and $\hat{r}_2^2$ is the normalized second moment of wing area. $\hat{r}_{2fly}^2$ and $\hat{r}_{2robot}^2$ differ slightly, due to a small null length at the base of the robotic wing required to accommodate the force sensor.

In this study, lift force is defined as the vertical component of the aerodynamics force on the wing; thrust force is the horizontal component; resultant is the vector sum of lift and thrust. Lift coefficient, thrust coefficient and resultant force coefficient are respectively defined in the following way, similar to (Wang and Sun, 2005):

$$C_l = L / [0.5 \rho U^2 (S_f + S_h)] \tag{3}$$

$$C_t = T / [0.5 \rho U^2 (S_f + S_h)] \tag{4}$$

$$C_r = R / [0.5\rho U^2 (S_f + S_h)] \tag{5}$$

L, T, and R denote the total lift, the total thrust and total resultant force. ρ is the density

of fluid; the reference velocity $U = 2\Phi n r_2 = 2.1\text{ms}^{-1}$; S_f and S_h are the areas of forewing

and hindwing, respectively.

Accordingly, we define lift coefficient, thrust coefficient and resultant force

coefficient for a single wing. For example, for forewing:

$$C_{l,f} = L_f / [0.5\rho U^2 (S_f + S_h)] \tag{6}$$

$$C_{t,f} = T_f / [0.5\rho U^2 (S_f + S_h)] \tag{7}$$

$$C_{r,f} = R_f / [0.5\rho U^2 (S_f + S_h)] \tag{8}$$

The total lift coefficient, total thrust coefficient and total resultant force

coefficient are as follows:

$$C_l = C_{l,f} + C_{l,h} \tag{9}$$

$$C_t = C_{t,f} + C_{t,h} \tag{10}$$

$$C_r = C_{r,f} + C_{r,h} \tag{11}$$

The lift coefficient on a dragonfly should be 2 times C_l, since it has two forewings

and two hindwings.

Detection for flow interaction mechanism

(Wang and Sun, 2005) and (Huang and Sun, 2007) proposed one reason for the

large decreases for the hindwing lift during forward flight with $\gamma = 180°\sim360°$ as follows:

the forewing downstroke produces a downwash behind it; when the hindwing lags the

forewing, it moves into the downwash and its angle of attack decreases, resulting in a reduction in aerodynamic force. (Maybury and Lehmann, 2004) suggested that forewing-hindwing interaction is probably due to two fluid dynamic phenomenons: LEV destruction and local flow condition. Here, we developed a measurement method to detect the local flow (upwash, downwash or vortex) generated by a wing, to give some direct proofs for the previous studies.
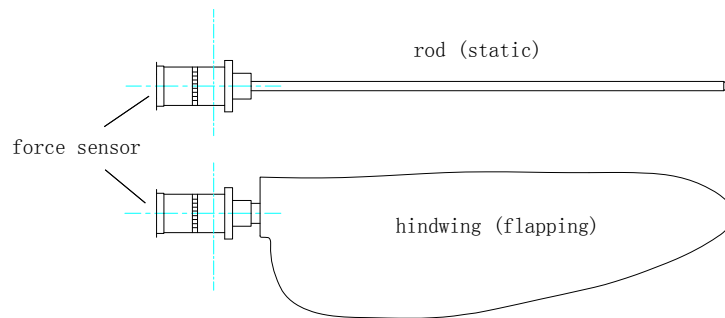

Fig. 4. Experiment setup to detect flow interaction mechanism. This an example to test interaction flow brought by hindwing. Forewing was replaced by a stationary rod.

Here is the method (Fig. 4): to investigate the influence from hindwing to forewing, we replace the forewing with a thin carbon fiber rod mounted with the sensor. The rod remain stationary while the hindwing flapping, and the sensor at the base of the rod measures instantaneous forces and torques acting on the rod by the flow due to hindwing moving. Similarly to the aerodynamic force measurements, the apparatus moves as a whole unit while taking measurements for forward flight cases. Likewise, to investigate the influence from forewing to hindwing, we simply replace the hindwing with the rod and repeat the experiments.

If there is an average downwash brought by the hindwing at any time instant, we can expect a force exerted on the rod due to the downwash. We make the rod to be thin (2.5 mm diameter) but long (the same length as forewing), because a thick rod will

15

change the flow field brought by the flapping hindwing. The only problem is that the force due to downwash would be very tiny, since the rod is thin and the downwash is probably not strong. Thus the signal to noise ratio will be low. Here we choose to use the torque measurements from the transducer, which is 100 times more sensitive than force measurement.

Results

Force measurements for anti-phase hovering

We first replay the hovering kinematics of *Aeshna juncea* (Norberg, 1975) on the robotic wings and measured lift and thrust forces on the both wings. Here the forewing and hindwing are anti-phase (180°), which is most commonly observed in dragonfly hovering flight. The results show an average lift force of 0.0711 N on the forewing and 0.082 N on the hindwing during one beat cycle. The average thrust forces are 0.001 N on the forewing and 0.003 N on the hindwing.

Here we can see that the combined average thrust forces are near zero when compared with the combined average lift forces of both wings, which is consistent with the hovering condition where the thrust should be zero.

We then apply equation (2) to scale the lift force back to those of a true dragonfly. The resulted average lift force is 187 mg on a forewing and 216 mg on a hindwing. The combined total lift on a four-wing dragonfly is therefore (187+216)*2=806 (mg). This result is comparable to the 754 mg body mass measured in (Norberg, 1972).

The time traces of instantaneous forces in two consecutive wingbeat cycles are shown in Fig. 5. Both forewing and hindwing produce lift peaks during downstrokes.

16

Because the flapping of forewing and hindwing are anti-phase, they generate lift force alternatively during one wingstroke. The average lift force on hindwing is 1.15 times that on forewing, while the area of hindwing is 1.32 times that of forewing. This inconsistency is probably caused by the fact that, compared to forewing, hindwing has more area distributed at positions close to the body. It was proposed that for dragonfly flight, the hindwing acts as power wing which provide more lift force while the forewing is the steering wing (Wang et al., 2003). Compared to the average lift force, the average thrust in hover is much smaller. As we can see, the total lift force is generated alternatively by the forewing and hindwing during one wingbeat, by doing so the insect is able to hover with regular forces which reduce the vibration of the body. Detailed evidence in shown in Fig. 7 with analysis followed in the next section.
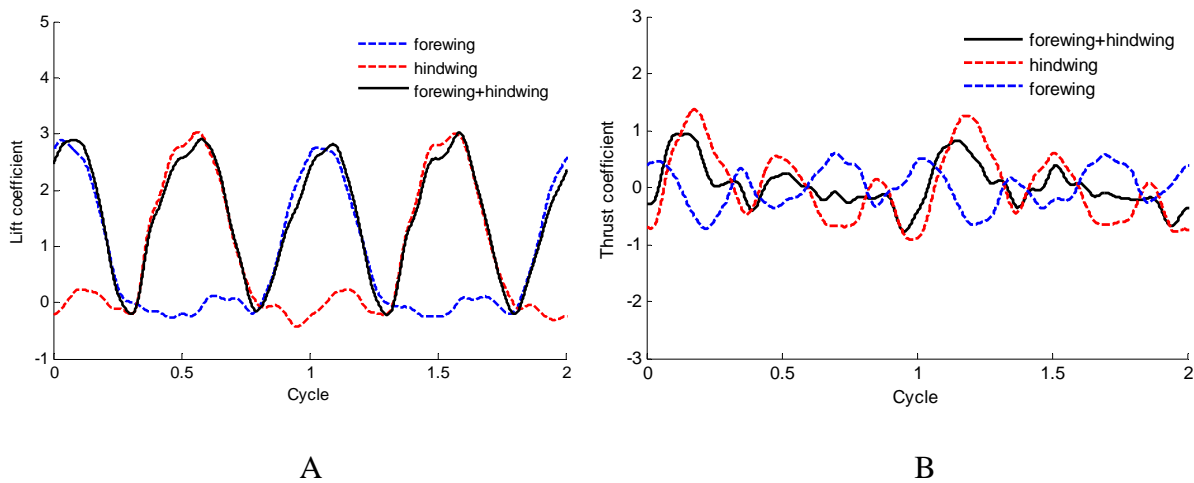

Fig. 5. Time trace of lift and thrust force coefficients generated when hovering with $\gamma = 180^\circ$. A, lift force coefficients on forewing, hindwing and total lift of the two; B, thrust force coefficients forewing, hindwing and total thrust of the two.

Effect of phase difference in hover

We measured the instantaneous forces with the same kinematics of hovering but

17

systematically vary the phase differences from 0° to 360° in steps of 30°. The average lift

coefficients, average thrust coefficients and average resultant force coefficients of the two

wings according to varying phase difference are plotted in Fig. 6.
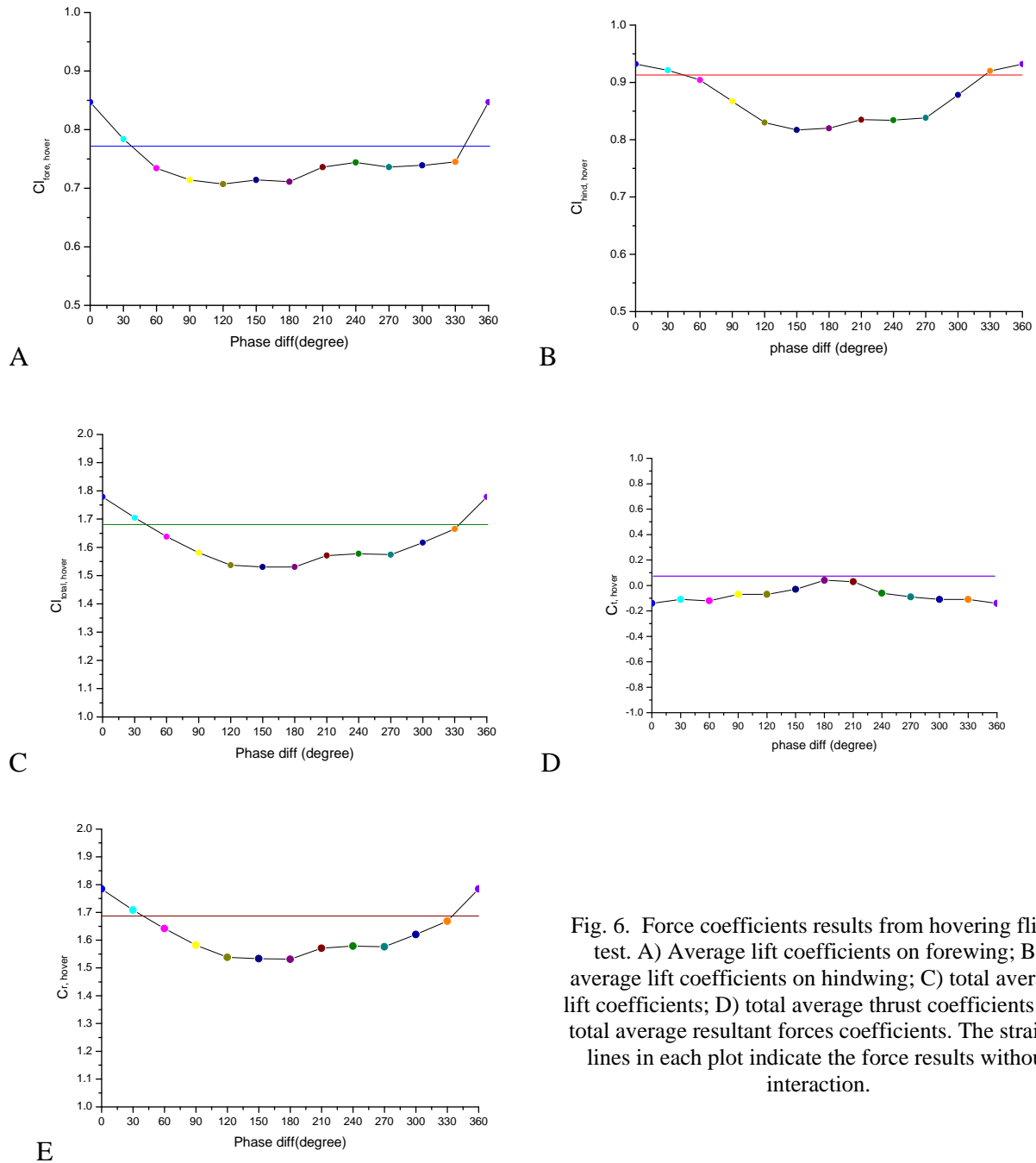

Fig. 6. Force coefficients results from hovering flight test. A) Average lift coefficients on forewing; B) average lift coefficients on hindwing; C) total average lift coefficients; D) total average thrust coefficients; E) total average resultant forces coefficients. The straight lines in each plot indicate the force results without interaction.

Fig. 6 shows the averaged force coefficients in hover. As the phase difference tends to 0°, forces tend to be higher, and reach their maximum on 0°. The forces get lower values when γ is around 180°. An interesting point is that not all values are below the single wing force, that is, the wing-wing interaction is not always detrimental to force generation. We can conclude here, in area 330°~30°, the wing-wing interaction enhances the total lift force by up to 6%; in area 150°~180°, interaction decreases the total lift force by up to 9%. The resultant force plot is almost identical to the lift force plot, just because thrust force is much smaller than vertical force, which is reasonable for a hovering case.

This part of study supplies a direct proof for the statement that in-phase flight generates larger aerodynamic forces than anti-phase flight, and also larger than the case without wing-wing interaction. This may explain the behavior that dragonfly flies in-phase in case of accelerating or maneuverings that calls for a high force generation. But why in-phase brings enhancement on lift force is still unclear. This problem will be discussed in later sections.
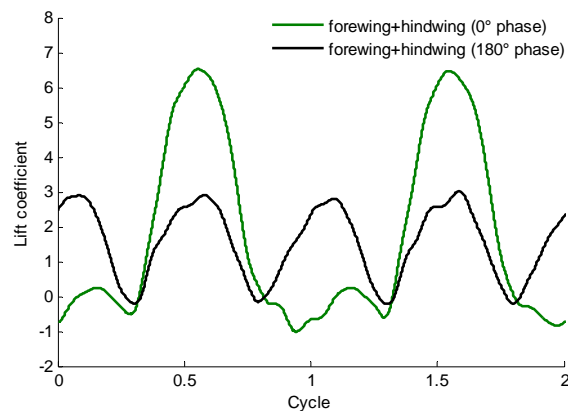

Fig. 7. Comparison between total lift forces generated when hovering with $\gamma = 0°$ and $\gamma = 180°$ respectively.

In order to find out the possible reason that dragonfly uses anti-phase style for

hovering mode, we need to compare the time traces of total lift forces generated by $\gamma = 0°$ with those generated by $\gamma = 180°$ (Fig. 7). It was noted that anti-phase produces uniform flight, whereas flight produced by in-phase stroking is irregular (Rüppell, 1989). Fig. 7 shows the instantaneous lift force coefficients comparison between in-phase and anti-phase flight. As we can see, in-phase brings larger irregularity in the aerodynamic forces than anti-phase does. Observing from the time trace curve for in-phase hovering, there exists a 1/2 cycle period when lift force is closed to zero, while in another 1/2 cycle the peak value is two times of the peak value for anti-phase flight, because forewing and hindwing peak overlap. This irregularity of instantaneous forces increases the body vibration when hovering, while for anti-phase flight the inequality can be compensated to some extent by evenly distributing the peak forces of forewing and hindwing on the whole cycle. Besides minimizing the force irregularities and keeping body posture stable, anti-phase flight can also save energy that might be lost in body vibration (Wang and Russell, 2007). Moreover, Usherwood and Lehmann showed that dragonfly can also save aerodynamic power during anti-phase hovering (Usherwood and Lehmann, 2008). Thus, it is reasonable that dragonflies would rather lose 15% (the gap between in-phase and anti-phase) force production for flight stability and vibration suppression as well as power efficiency.

Effect of phase difference in forward flight

Although no specific kinematics are available for *Aeshna juncea*, (Norberg, 1975) pointed out that in forward flight, the body is also kept horizontal, and horizontal and vertical winds seem not to make any significant change on the data. Thus, we assume that

20

in forward flight, the stroke plane is kept at 60°, frequency is still 36 Hz, stroke angle

does not change, and a J=0.35 advance ratio (a medium speed) is used here. The changed

parameter might be the angle of attack. Our strategy is to adjust the extreme rotation

angles of the model wings when they are flapping forward in 90° phase difference, to

balance the body weight 754 mg as well as the body drag at J=0.35. 90° is used as the

calibration phase difference, because 54-100° are typically used for forward flight. The

body-drag of Aeshna juncea is not available. Here, the body-drag coefficients for

dragonfly *Sympetrum sanguineum* (Wakeling and Ellington, 1997) are used, that is about

0.03 at 0.35 advance ratio.

Similarly to the hovering case, we tested the wing aerodynamics by varying phase

difference systematically in steps of 30°. The average lift coefficients, average thrust

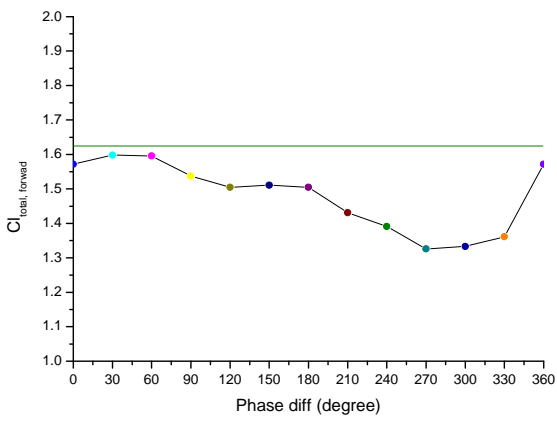coefficients and average resultant force coefficients of the two wings are plotted below

(Fig. 8).

As seen in Fig. 8, during forward flight, interaction patterns for forewing and

hindwing differ a lot. Note that the interaction always enhances the forewing's force

generation no matter how much γ is, while the hindwing always loses force production

because of the interaction. Lift on forewing is enhanced by at most 23% when flapping

in-phase and at least 4% when phase difference falls into (120°~330°); Lift on hindwing

reaches maximum on 60° and minimum on 270°. Hindwing is subjected to a severe loss

on force production up to 38% due to the interaction with forewing.
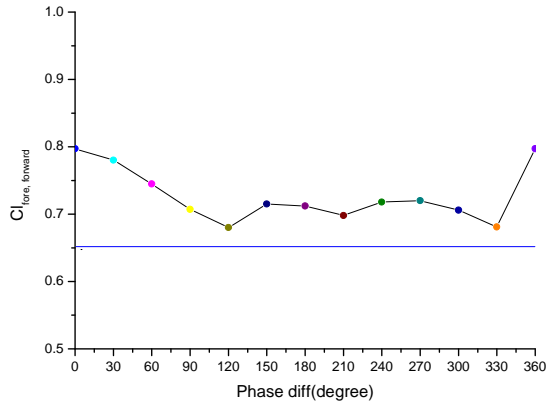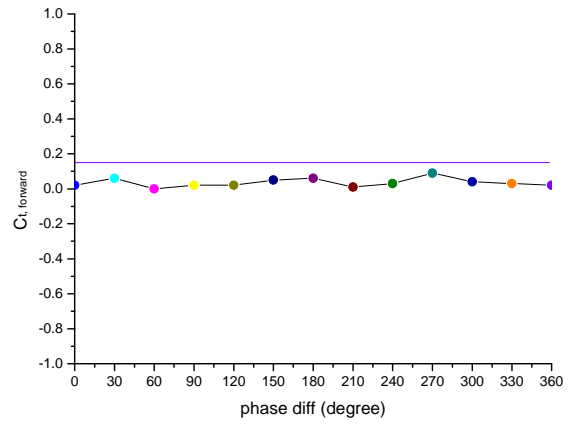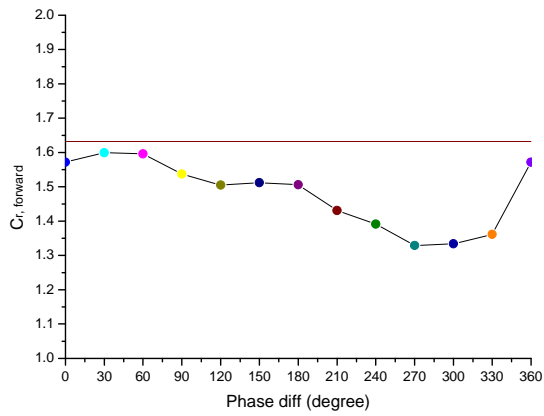
A
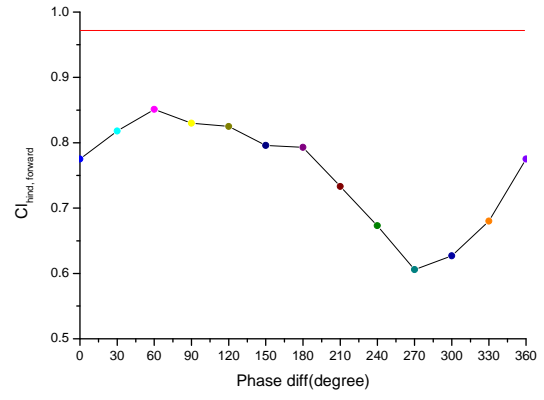
B

C

D

E

Fig. 8. Force coefficients results from forward flight test. A) lift coefficients on forewing; B) lift coefficients on hindwing; C) total lift coefficients; D) total thrust coefficients; E) total resultant forces coefficients. The straight lines in each plot indicate the force results without interaction.

The total force on two wings does not lose so much force as the hindwing does, due to the considerable enhancement on forewing lift. It is obvious to distinguish the case around 90° and the case around 270°: the former one can offer dragonfly an 18% higher force than the latter one. At the same time, 270° offers similar vibration and stability properties as 90°. This may explain why dragonfly never favors the 270° phase difference.

The above results agree qualitatively with the CFD results from (Wang and Sun, 2005) and (Huang and Sun, 2007) to some extent. Their conclusion is that the forewing is only slightly influenced by the wing–wing interaction, but the hindwing lift is greatly reduced by 20~60% during forward flight with a 180°~360° phase difference, compared with that of a single hindwing. In our results, furthermore, there are obvious lift enhancements on the forewing.

For thrust force measurement, (Warkentin and DeLaurier, 2007) conducted a systematic series of wind-tunnel tests on an ornithopter configuration consisting of two sets of symmetrically flapping wings, located one behind the other in tandem. It was discovered that the tandem arrangement can give thrust increases over a single set of flapping wings for certain relative phase differences and longitudinal spacing between the wing sets. In particular, close spacing on the order of one chord length is generally best, and phase differences of approximately $0°\pm50°$ give the highest thrusts and propulsive efficiencies. Nevertheless, this conclusion does not apply for the dragonfly flight. Instead, the thrust plot above indicates a drop on thrust force caused by interaction, no matter what the phase difference is. This would be reasonable if we notice that the space between forewing and hindwing of dragonfly is much smaller that the one chord spacing between the ornithopter wing sets.

Discussions

Our force results show not only the negative effect but also positive effect for the aerodynamic force on both wings. In order to explain the mechanism of interaction, we try to detect local flow conditions (upwash, downwash or LEV) brought by a flapping wing in the following experiments.

Interaction flow produced by forewing

We first study the interaction from forewing to hindwing. In the case of hovering flight, the lift force on hindwing reaches minimum with $\gamma=180°$; while in the case of forward flight, the lift force on hindwing reaches minimum with 270° phase difference. In Fig. 9, we compare the time traces of lift force to find out in which time period the instantaneous forces are changed by interaction from forewing.
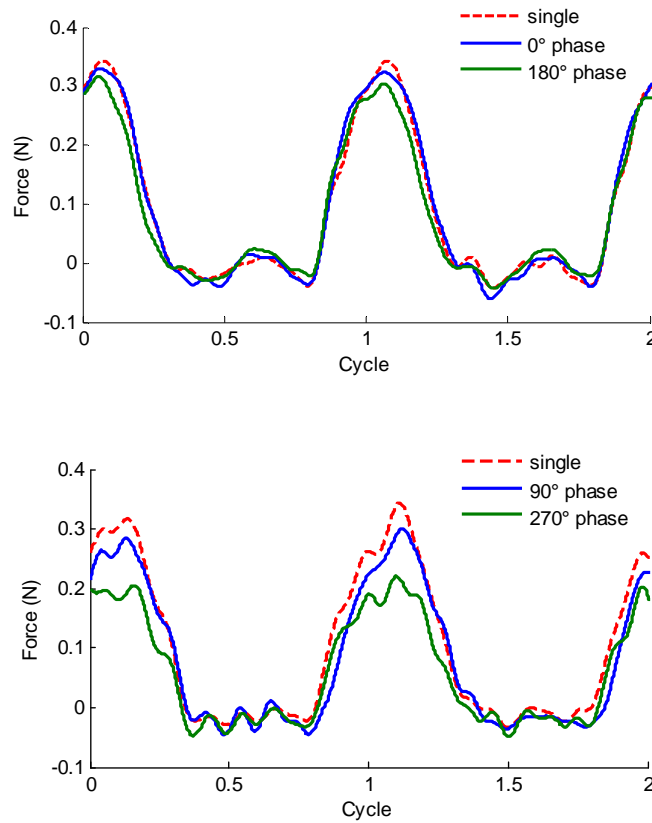
Fig. 9. Comparison of hindwing lift with/without forewing interaction in hover (A) and forward flight (B).

From the Fig. 9, we conclude that the interaction from forewing mainly decrease lift force on hindwing when hindwing is in the midway of downstroke. This is reasonable because a large portion of lift is produce during this period, since wings reach the highest flapping speed and largest angle of attack around the midway of downstroke. Thus, we expect to detect some downwash at the position of midway flapping angle.

We replaced the hindwing with a thin rod, and adjust it into the position of midway flapping angle, keep it static while make the forewing flapping, measure the instantaneous forces and torques generated on the rod in the mean time. The results are shown in Fig. 10.
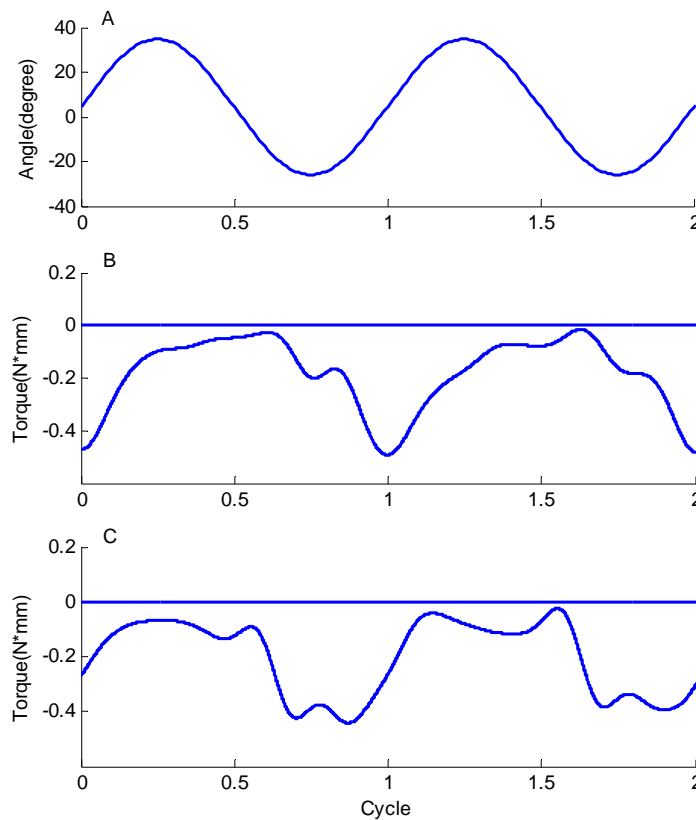

Fig. 10. Instantaneous torque on the rod generated by forewing interaction. A is the translational angle of forewing; B is for hovering flight; C is for forward flight. Negative value means a downward flow. The horizontal straight line is for zero reference.

Generally, a downward torque on the rod indicates a downward flow passing by the rod, and the higher the torque, the higher the flow strength. Based on this assumption, results in Fig. 10 show that: in hovering flight, interaction from forewing always generates, to some extent, a downward flow at the position of the rod. The strength of the flow reaches maximum when forewing is in the midway of upstroke. Now we are ready to explain why hindwing receive minimum lift with 180° phase difference when hovering: with 180° phase difference, hindwing approaches the midway of downstroke while forewing approaches the midway of upstroke, and at this moment, the strongest downward flow appears; with other phase difference, for example 0°, hindwing approaches the midway of downstroke when forewing also approaches the midway of downstroke, but the downward flow at this moment is almost eliminated, according to Fig. 10.

The same mechanism applies for forward flight case. The interaction from forewing generates comparatively stronger downward flow when forewing is in a position below the midway point than above the midway point. If γ falls in 180~360°, hindwing arrives at its midway of downstroke just as a stronger downward flow is generated by forewing. Thus, in forward flight, hindwing obtains lower lift force with 180~360° phase difference than 0~180° phase difference.

Our results in this subsection agree with (Huang and Sun, 2007) well. They showed a flow field caused by a flapping forewing by using CFD method, and found that the forewing in each of its downstroke produces a downwash behind it. Here, we give the proof for the existence of such a downwash, by detecting the flow.

Interaction flow produced by hindwing

Although forewing and hindwing share the same the kinematics, we expect to observe different interaction flow from hindwing, compared with interaction flow from forewing. There are three reasons for that. First, the arrangement of the wings is not symmetric, for that the leading edge of hindwing is close to the trailing edge of forewing, while the leading edge of forewing is far from the trailing edge of hindwing. This makes it possible that the leading edge vortex (LEV) of hindwing plays an important role in interaction mechanism, but the LEV of forewing can hardly affect hindwing. Second, during forward flight, hindwing runs toward the "jet" area of forewing, but forewing escapes that of hindwing. Thus, we can expect that the interaction from hindwing is much smaller that interaction from forewing in forward case. Third, the fore measurements show that in many cases the lift on forewing is enhanced by interaction, which suggests there might be some upwash coming from the hindwing.

Fig. 11 shows the instantaneous forces on forewing during hovering and forward flight. We can see that the interaction from hindwing mainly decrease or enhance lift force on forewing when forewing is in the midway of downstroke. Thus, we expect to detect some downwash or upwash at the position of midway downstroke of forewing.

We again replaced the forewing with a thin rod, and adjust it into the position of midway flapping angle, keep it static while make hindwing flapping, measure the instantaneous force generated on the rod in the mean time. The results are shown in Fig. 12.

As we expected, different phenomenon from the interaction from forewing shows up (Fig. 12): (i) a sharp upwash was detected; (ii) the upwash occurs immediately after

hindwing passes the midway position in downstroke and lasts for a short time; (iii) a mild

flow in a much smaller strength takes up most time of a cycle. It seems from Fig. 12 that

the interaction flow from hindwing is a sum of two parts: a sharp upwash and a mild flow.
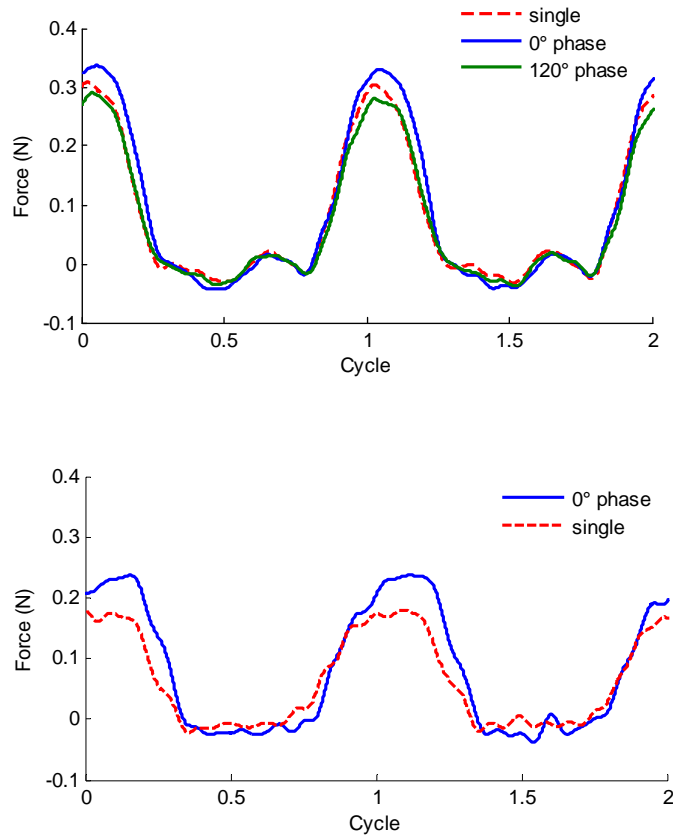

Fig. 11. Comparison of time trace of forewing lifts in cases of with/without hindwing interaction. A is for hovering flight; B is for forward flight.

Considering that the down stroking hindwing brings strong downward

momentum to the fluid around, one may expect a sharp downwash at the rod position

when hindwing passes the rod. But the fact is opposite: there is a sharp upwash. Thus,

here comes an interesting problem how the upwash is generated. Noticing that the sharp

upwash always occurs immediately after hindwing passes the rod and does not last long,

we may propose that this sharp upwash is probably relevant to the formation of LEV of hindwing, as depicted in Fig. 13. During the downward movement of hindwing, a high pressure area is formed below hindwing and a low pressure area is formed above hindwing. Then, the pressure difference drives fluid flowing from below to above, meanwhile passing the rod. Finally the LEV is formed.
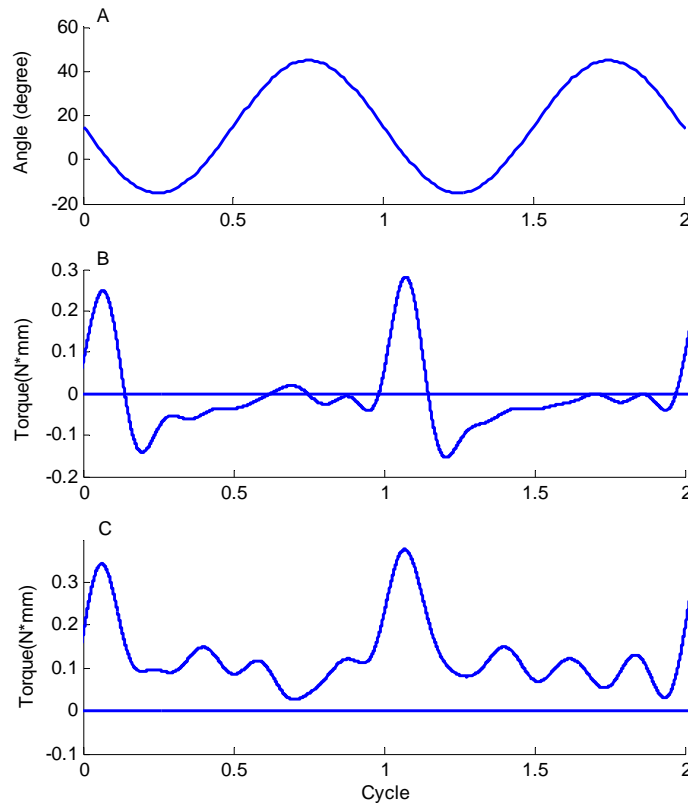

Fig. 12. Instantaneous torque on the rod generated by hindwing interaction. A is the translational angle of hindwing; B is for hovering flight; C is for forward flight. Positive value means an upward force. The horizontal strait line is for zero reference.

There are some other proofs for the relationship between LEV and wing-wing interaction. (Reavis and Luttges, 1988) observed flow field produced by a tethered dragonfly and found that the appearance of vortex structures was coincident in time with increasing lift. This means the vortex appears at the beginning of downstroke, since at

this moment, lift also starts to increase. (Lu and Shen, 2008) identified the substructures of the LEV system on flapping wings, by utilizing an electromechanical model dragonfly wing flapping in a water tank and applying a digital stereoscopic particle image velocimetry (DSPIV) to measure the target flow fields. (Saharon and Luttges, 1989) also suggested that lift force could be enhanced by constructive flow interactions terms of integrating or fusing of vortex structures. All these statements indicate a strong connection between the lift enhancement and the existence of LEV. Moreover, in horizontal stroke plane study, (Maybury and Lehmann, 2004) gave a reasonable explanation for lift decrease on hindwing when forewing leads hindwing 1/4 cycle: The smaller LEV on the hindwing coincides with the attenuation of lift when forewing leads by1/4 cycle. This interaction mechanism is called LEV destruction, which is quite different from that for inclined stroke plane flight in the present study: the LEV enhances lift by means of sharp upwash (Fig. 13).
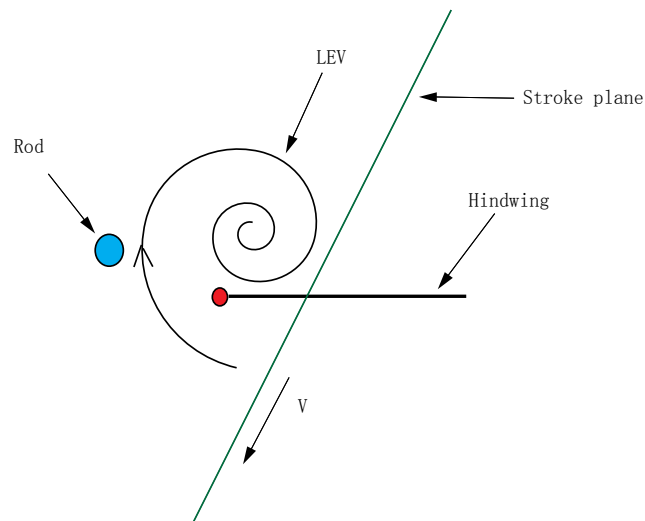

Fig. 13. A possible formation mechanism for sharp upwash, as a result of leading edge vortex.

Since the sharp upwash is brought by LEV, the interaction from sharp upwash, together with interaction from LEV destruction (Maybury and Lehmann, 2004) can be classified as 'LEV interaction'. In the rod test, sharp upwash appears for a short time in each stroke cycle (Fig. 12). But for wing-wing interaction, the sharp upwash can take effect for a much longer time. This is because when two wings flap together with a phase difference close to 0°, the forewing always keeps close to the leading edge of hindwing during the whole downstroke, therefore, sharp upwash acts on forewing all through the downstroke period. Sharp upwash acts on the rod for only a short time just because the rod does not move together with hindwing. With enhancement from LEV interaction, lift force with 0° phase difference can reach the maximum value. This might insightfully explain the dragonfly's behavior that they fly in 0° phase difference when accelerating or maneuvering.

If phase difference is not close enough to 0°, then LEV interaction will disappear, then the lift on forewing will be affected only by a mild flow interaction (local flow interaction), which increases lift slightly when the mild flow is upward and reduces lift when the mild flow is downward.

Conclusions

The experiments described here investigate the effect of forewing-hindwing interactions in dragonflies during hovering and forward flight with inclined stroke planes. Overall, wing-wing interaction is detrimental to total lift force generation. However, forewing generated more lift in forward flight due to the interaction from the LEV of the hindwing causing an upwash. Hindwing lift was significantly reduced in forward flight

due to the downwash from forewing. In-phase flight generates higher lift than other phase differences, while 270 phase difference generates the lowest lift. In hovering, dragonflies use anti-phase flight which generates a regular lift force for stability and vibration reduction purposes.

Acknowledgements

List of symbols

C_l	dimensionless lift coefficient
C_t	dimensionless thrust coefficient
C_r	dimentionless resultant coefficient
$C_{l,f}$	dimensionless lift coefficient for forewing
$C_{t,f}$	dimensionless thrust coefficient for forewing
$C_{r,f}$	dimentionless resultant coefficient for forewing
$C_{l,h}$	dimensionless lift coefficient for hindwing
$C_{t,h}$	dimensionless thrust coefficient for hindwing
$C_{r,h}$	dimentionless resultant coefficient for hindwing
$F_x^*(t)$	wing inertia force m
I_f	moment of inertia for forewing
I_h	moment of inertia for hindwing
J	advance ratio
m	mass of insect
m_w	mass of insect wing
n	wing beat frequency
l_x	first moment arm of wing mass center in x direction
l_y	first moment arm of wing mass center in y direction
LEV	leading edge vortex
L	lift force
T	thrust force
R	resultant force

L_f	lift force on forewing
T_f	thrust force on forewing
R_f	resultant force on forewing
L_h	lift force on hindwing
T_h	thrust force on hindwing
R_h	resultant force on hindwing
r	wing length
r_f	forewing length
r_h	hindwing length
Re	Reynolds number
S_f	forewing area
S_h	hindwing area
$\hat{r}^2(S)$	Non-dimensional second moment of area
U	mean linear wing velocity
υ	dynamic viscosity of fluid
Φ	stroke amplitude
ϕ_f	translational angle of forewing
ϕ_h	translational angle of hindwing
ρ	fluid density
β	stroke plane angle
γ	phase difference (hindwing leads forewing)

Appendix

Table A1. Parameters of dragonfly and robotic model

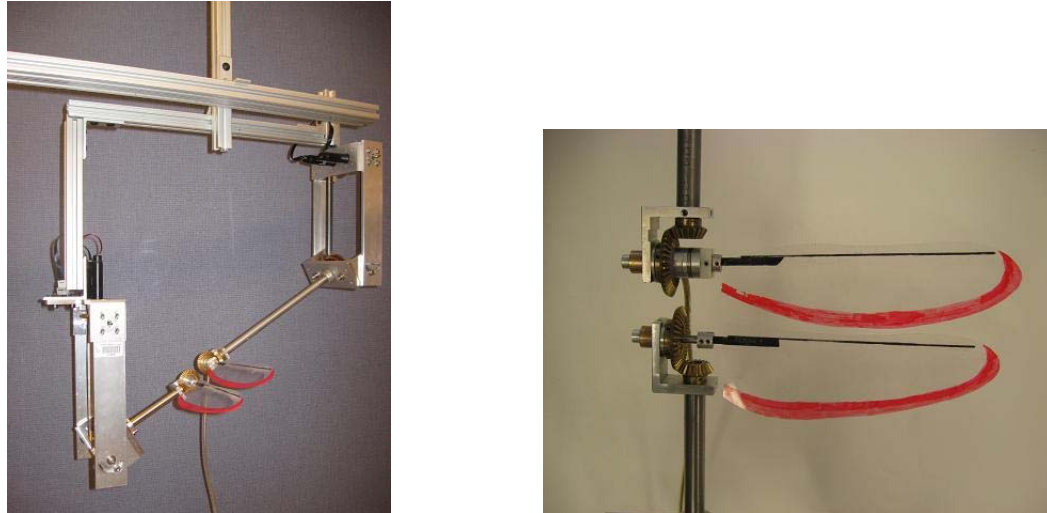|	β	n	r_f	r_h	ϕ_f	ϕ_h	Re
Dragonfly	60°	36Hz	4.74 cm	4.60 cm	-25°~35°	-15°~45°	1160
Robotic model	60°	0.5Hz	19 cm	18.5 cm	-25°~35°	-15°~45°	1160

Figure A1: Experimental setup.

Reference

Alexander, D. E. (1984). Unusual phase relationships between the forewings and hindwings in flying dragonflies. *J Exp Biol* **109**, 379-383.

Appleton, F. M. (1974). Dragonflies and flight. *Nature Canada* **3(3)**, 25-29.

Azuma, A., Azuma, S., Watanabe, I. and Furuta, T. (1985). Flight mechanics of a dragonfly. *J Exp Biol* **116**, 79-107.

Azuma, A. and Watanabe, T. (1988). Flight performance of a dragonfly. *J Exp Biol* **137**, 221-252.

Dickinson, M. H., Lehmann, F. O. and Sane, S. P. (1999). Wing rotation and the aerodynamic basis of insect flight. *Science* **284**, 1954-60.

Fry, S. N., Sayaman, R. and Dickinson, M. H. (2005). The aerodynamics of hovering flight in Drosophila. *J Exp Biol* **208**, 2303-18.

Huang, H. and Sun, M. (2007). Dragonfly forewing-hindwing interaction at various flight speeds and wing phasing. *AIAA J.* **45**, 508-511.

Lan, C. E. (1979). The unsteady quasi-vortex-lattice method with applications to animal propulsion. *J. Fluid Mech.* **93**, 747-765.

Lu, Y. and Shen, G. X. (2008). Three-dimensional flow structures and evolution of the leading-edge vortices on a flapping wing. *J Exp Biol* **211**, 1221-1230.

Maybury, W. J. and Lehmann, F. O. (2004). The fluid dynamics of flight control by kinematic phase lag variation between two robotic insect wings. *J Exp Biol* **207**, 4707-26.

Norberg, R. A. (1972). The pterostigma of insect wings and inertial regulator of wing pitch. *J. Comp. Physiol* **81**, 9-22.

Norberg, R. A. (1975). Hovering flight of the dragonfly: Aeschna juncea L., kinematics and aerodynamics. *Swimming and Flying in Nature* **2**, 763-780.

Reavis, M. A. and Luttges, M. W. (1988). Aerodynamic forces produced by a dragonfly. *AIAA J.* **88-0330**, 1-13.

Rüppell, G. (1989). Kinematic analysis of symmetrical flight manoeuvres of odonata. *J Exp Biol* **144**, 13-42.

Saharon, D. and Luttges, M. W. (1989). Dagonfly unsteady aerodynamics: The role of the wing phase relationship in controlling the produced flows. *AIAA J.* **89-0832**, 1-19.

Thomas, A. L., Taylor, G. K., Srygley, R. B., Nudds, R. L. and Bomphrey, R. J. (2004). Dragonfly flight: free-flight and tethered flow visualizations reveal a diverse array of unsteady lift-generating mechanisms, controlled primarily via angle of attack. *J Exp Biol* **207**, 4299-323.

Usherwood, J. R. and Lehmann, F. O. (2008). Phasing of dragonfly wings can improve aerodynamic efficiency by removing swirl. *J R Soc Interface*.

Wakeling, J. and Ellington, C. (1997). Dragonfly flight. I. Gliding flight and steady-state aerodynamic forces. *J Exp Biol* **200**, 543-556.

Wang, H., Zeng, L., Liu, H. and Yin, C. (2003). Measuring wing kinematics, flight trajectory and body attitude during forward flight and turning maneuvers in dragonflies. *J Exp Biol* **206**, 745-57.

Wang, J. K. and Sun, M. (2005). A computational study of the aerodynamics and forewing-hindwing interaction of a model dragonfly in forward flight. *J Exp Biol* **208**, 3785-804.

Wang, Z. J. (2004). The role of drag in insect hovering. *J Exp Biol* **207**, 4147-55.

Wang, Z. J. and Russell, D. (2007). Effect of forewing and hindwing interactions on aerodynamic forces and power in hovering dragonfly flight. *Physical Review Letters* **99**, -.

Warkentin, J. and DeLaurier, J. (2007). Experimental aerodynamic study of tandem flapping membrane wings. *AIAA J.* **44**, 1653-1661.

Whitehouse, F. C. (1941). British Columbia dragonflies (Odonata), with notes on distribution and habits. *The American Midland Naturalist* **26(3)**, 488.